Journal of Catalysis **207,** 361–370 (2002)
doi:10.1006/jcat.2002.3534, available online at http://www.idealibrary.com on IDEAL®

# Formation and Catalytic Properties of Edge-Bonded Molybdenum Sulfide Catalysts on $TiO_2$

Yasuhiro Araki,* Kosaku Honna,* and Hiromichi Shimada†,[1]

*Tsukuba Branch of Advanced Catalysts Research Laboratory, Petroleum Energy Center, 1-1 Higashi, Tsukuba, Ibaraki 305-8565, Japan; and †National Institute of Advanced Industrial Science and Technology (AIST), 1-1-1 Higashi, Tsukuba, Ibaraki 305-8561, Japan

Received October 19, 2001; revised December 28, 2001; accepted December 28, 2001

**The effect of preparation conditions (calcination atmosphere, sulfidation atmosphere, and sulfidation temperature) on the orientation of $MoS_2$ clusters on $TiO_2$ supports was studied. Edge-bonded $MoS_2$ clusters formed when the catalyst was sulfided in a flow of $H_2S/N_2$ at 573 or 673 K. However, when sulfided in $H_2S/N_2$ at higher temperatures than 773 K, the edge-bonded $MoS_2$ clusters transformed to highly aggregated basal-bonded $MoS_2$ clusters. Catalytic activity tests, using hydrogenation of 1-methylnaphthalene as a model test reaction, revealed that the turnover frequency on the catalyst with edge-bonded $MoS_2$ clusters prepared by sulfiding at 573 K in $H_2S/N_2$ was higher than that on the catalyst with basal-bonded $MoS_2$ clusters prepared by sulfiding in $H_2S/H_2$.** 

*Key Words:* **hydrodesulfurization (HDS) catalysts; catalyst dispersion; morphology; orientation.**

## INTRODUCTION

Alumina-supported Mo sulfide catalysts with Co or Ni as promoter are widely called *hydrodesulfurization* (HDS) catalysts and have long been used for hydrotreatment of petroleum fractions. Within the past decade, the catalytic performance of HDS catalysts has been significantly improved to satisfy a wide range of requirements. The most recent requirement is to drastically reduce the sulfur level in diesel fuels, to at least below 30 ppm, to meet more stringent environmental regulations that will be introduced in the near future. Such reduction in sulfur (deep desulfurization) requires that next-generation HDS catalysts possess the ability to remove sulfur from *hard-to-desulfurize* compounds such as 4,6-dimethyldibenzothiophene (1–3). This ability requires the development of HDS catalysts that have full dispersion of highly active catalytic sites. In addition, high hydrogenation activity as well as high HDS activity are required for such deep desulfurization catalysts to eliminate the steric hindrance that lowers the reactivity of the above hard-to-desulfurize compounds.

In the late 1980s, Topsøe *et al.* (4) proposed that the active catalytic sites of Co- or Ni-promoted Mo sulfide catalysts are located on the so-called "Co (Ni)–Mo–S" structure, in which Co (Ni) atoms are bonded to the edges of $MoS_2$ crystallites. Later, Topsøe *et al.* (5) suggested that there are different types of "Co–Mo–S" structures and that only some of these Co–Mo–S structures function as highly active catalytic sites in industrial catalysts. Therefore, the Co–Mo–S structures on the support must be clarified in detail and the catalytic activities of those structures must be determined.

Numerous studies indicate that the catalytic activity of Co–Mo–S structures depends on the morphology of the $MoS_2$ clusters on the support, because the layered $MoS_2$ structure is highly anisotropic. Candia *et al.* (6) claimed that there are at least two types of Co–Mo–S structures: one called "Co–Mo–S(I)," which has relatively strong interaction with the support and is less catalytically active than the other structure, called "Co–Mo–S(II)," which has weak interaction with the support (7–12). Single-layered $MoS_2$ clusters with Co at their edges probably are Co–Mo–S(I), whereas multilayered $MoS_2$ clusters with Co, except on the bottom layer, are Co–Mo–S(II). Whitehurst *et al.* (13) suggested that, due to steric hindrance, the bottom layers of Co–Mo–S structures that have multilayers might be less active than the other layers. Vrinat *et al.* (14) reported that in Mo sulfide catalysts without Co promoters, only the topmost layers of $MoS_2$ clusters on the support are catalytically active in the HDS reaction of thiophene. Furthermore, Daage *et al.* (15) claimed that all the edge planes of $MoS_2$ clusters possess HDS activity, whereas due to steric hindrance, only the "rim," i.e., the top and bottom edges, of unsupported $MoS_2$ clusters possess hydrogenation activity. These three studies indicate that the morphology of $MoS_2$ clusters, in particular the aspect ratio of the layered structure (i.e., lateral dimension/thickness), significantly affects the catalytic performance, irrespective of the presence or absence of Co- or Ni-promoters.

Based on the above discussion, the catalytic performance of Co–Mo–S structures depends also on the orientation of the $MoS_2$ clusters on the support, because the upper edge sites of the "edge-bonded" $MoS_2$ clusters that are

[1] To whom correspondence should be addressed. Fax: +81-298-61-2371. E-mail: h-shimada@aist.go.jp.



0021-9517/02 $35.00

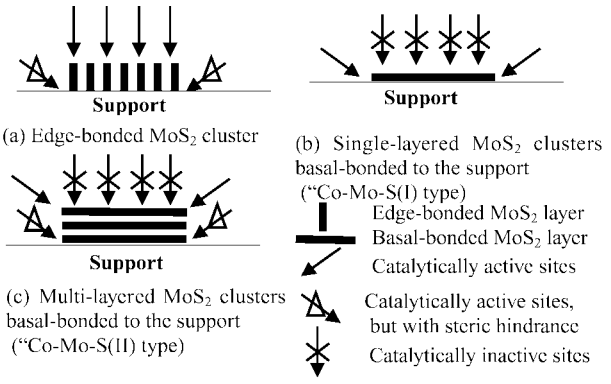


**FIG. 1.** Schematic of the orientation of $MoS_2$ clusters on supports.

perpendicular to the support surface (Fig. 1a) have weaker electronic interaction with the support than do single-layered $MoS_2$ clusters that are "basal-bonded" (parallel) to the support (Fig. 1b). In addition, the upper edge sites of the edge-bonded $MoS_2$ clusters have less steric hindrance than do either the edge sites of the basal-bonded single-layered $MoS_2$ clusters (Fig. 1b) or the edge sites of the bottom layers of the basal-bonded multilayered $MoS_2$ clusters (Fig. 1c).

Until recently, no clear evidence was reported for such edge-bonded $MoS_2$ clusters on $\gamma$-$Al_2O_3$, although there were some discussion about the edge-bonded $MoS_2$ clusters based on transmission electron microscopy (TEM) pictures (16–18). In 1999, using $\gamma$-$Al_2O_3$ single crystals with different indices, Sakashita and Yoneda (19) showed that there is an epitaxial relationship between the orientation of $MoS_2$ clusters and the surface structures of $\gamma$-$Al_2O_3$; namely, when the spacing of $MoS_2$ layers is identical to the lattice distance of a surface plane of an $\gamma$-$Al_2O_3$ crystal, $MoS_2$ clusters are edge-bonded to the surface. As a result, edge-bonded clusters form on (100) $\gamma$-$Al_2O_3$, whereas basal-bonded $MoS_2$ clusters form on other planes, such as (111) and (110), or on amorphous planes of $\gamma$-$Al_2O_3$. In a subsequent study, Sakashita *et al.* (20) confirmed an epitaxial relationship for the orientation of $MoS_2$ clusters on anatase-type $TiO_2$ powders; namely, edge-bonded $MoS_2$ clusters form on the spherical anatase powders that mainly expose the (001) plane.

In our current study, we determined the preparation conditions (calcination atmosphere, sulfidation atmosphere, and sulfidation temperature) that enhance the formation of edge-bonded $MoS_2$ clusters on an anatase-type $TiO_2$ support. First, we clarified the effects of calcination, either in nitrogen or dry air, and the sulfidation conditions, using either $H_2S/N_2$ or $H_2S/H_2$ at temperatures ranging from 573 to 873 K, on the orientation of $MoS_2$ clusters on the support. Then, we compared the catalytic activities of these prepared $MoS_2$-supported catalysts using a model test reaction. We chose the hydrogenation of 1-methylnaphthalene (1-MN) as a model test reaction, because more prominent effects of edge-bonded clusters are expected in the hydrogenation of aromatic rings, in which the effect of steric hindrance is larger than in the HDS reactions. Finally, we clarified the characteristics of the edge-bonded and basal-bonded $MoS_2$ clusters needed in the design of highly active catalytic sites.

## EXPERIMENTAL

### *Catalyst Preparation*

The $TiO_2$ support used here was ultrafine anatase-type particles (Nanophase Technologies Ltd.) with an average particle diameter of 30 nm, a BET surface area of 50 $m^2/g$, and a purity of 99.95%. The Mo sulfide catalysts were prepared by using an equilibrium adsorption method (21, 22). In the equilibrium adsorption, 10 g of the $TiO_2$ powder was mixed with 400 $cm^3$ of an aqueous solution of $(NH_4)_6Mo_7O_{24}$ (0.007 M) and kept at 323 K for 24 h. The pH of the solution was kept constant at 2.0 by adding $HNO_3$. The pH value of 2.0 for equilibrium adsorption was chosen to achieve high loading of molybdate on the $TiO_2$ support but to not exceed too much that of the monolayer coverage.

After filtration and rinsing with pure water, the solid was dried in air at 298 K for 16 h and then at 323 K for 3 h. The calcination was done at 723 K for 3 h in a flow of either nitrogen or dry air to clarify the effect of the inert-gas atmosphere that was used in the previous study (20) on the morphology and orientation of $MoS_2$ clusters on the support. Sulfidation of the resulting calcined catalysts was done for 2 h at various temperatures, ranging from 573 to 873 K, in a flow of either 5% $H_2S/H_2$ or 5% $H_2S/N_2$. Induced coupled plasma emission spectrometry analysis indicated that the Mo loading was 4.6 wt% as metal.

### *Catalyst Characterization*

Observation of the catalysts after sulfidation was carried out using transmission electron microscopy (TEM) with a Hitachi H-800 operated at an accelerated voltage of 200 kV. Each catalyst sample was ground into powder (by using a mortar and a pestle) and then ultrasonically dispersed on a copper grid with holey carbon films in *n*-heptane.

X-ray photoelectron spectroscopy (XPS) spectra were obtained by using a PHI 5500 photoelectron spectrometer with monochromatic Al $K\alpha$ excitation (1486.6 eV, 150 W). The energy scale of the spectrometer was calibrated using the Au $4f_{5/2}$ (84.0 eV) line of a pure Au plate and the Cu $2p_{3/2}$ (932.4 eV) line of a sputtered Cu plate. All peak energies were corrected using the C 1s line of the adventitious carbon at 285.0 eV. As a reference for the assignment of S 2p lines, amorphous $MoS_3$ was prepared by thermal decomposition of ammonium-tetrathiomolybdate at 523 K for 1 h in a flow of $N_2$ according to a method in the literature (23, 24).

The dispersion of $MoS_2$ on the support was measured by using a NO chemisorption method. After being sulfided in a stream of either 5% $H_2S/H_2$ or 5% $H_2S/N_2$, about 0.2 g of the catalyst was treated with a flow of $H_2$ for 1 h at 603 K. Then, 10% NO/He pulses, each having a volume of 2.1 $cm^3$, were introduced to the catalyst at 303 K. The amount of NO at the exit of the reactor was monitored using a thermal conductivity detector so that saturation of the adsorption of NO on the catalyst could be detected.

*Catalytic Activity Test*

Catalytic activity was evaluated by using hydrogenation of 1-MN as a model test reaction. Before use, 1-MN was purified by column chromatography to remove N- and S-containing compounds in the reagent. The reactions were carried out at 603 K for 1 h in a microautoclave (inner volume of 35 $cm^3$) containing 10 $cm^3$ of the feed (25 wt% 1-MN with the balance being tetradecane) and hydrogen with an initial pressure of 6 MPa at 298 K. The feed and product were analyzed by using gas chromatography with a HP Ultra #1 capillary column. The reaction rate constants were calculated using the conversion data obtained for different amounts of the catalyst, ranging from 0.05 to 0.5 g, and assuming a pseudo-first-order kinetics. To apply this assumption, the reaction conditions were determined so that the total conversion would not exceed 20%. Under these conditions, decreases in the hydrogen partial pressure during the reactions were negligible. The products obtained were only 1- and 5-methyltetralin.

## RESULTS AND DISCUSSION

*Catalyst Characterization*

Figure 2 shows representative TEM images of $Mo/TiO_2$ catalysts sulfided in $H_2S/H_2$ at 573, 673, or 773 K after calcination in air. The catalysts sulfided at 573 and 673 K (Figs. 2a and 2b) had small numbers of $MoS_2$ clusters as a monolayer or as two layers (indicated by arrows in Fig. 2a). All of the layers were parallel to the surface of $TiO_2$, indicating basal-bonding on the support. Because the Mo loading was 4.6% (see Section Catalyst Preparation above), the major part of the Mo species was not detected in these images. This can be attributed either to high dispersion of $MoS_2$ clusters that contain fewer than seven Mo atoms per layer (25) or to insufficient sulfidation, particularly in the catalysts sulfided at 573 K. The catalyst sulfided at 773 K (Fig. 2c) had many $MoS_2$ clusters with multilayered structures (indicated by an arrow), indicating that aggregation and stacking of $MoS_2$ layers was proceeded by higher-temperature sulfidation. Note that Mo loading of 4.6% as metal corresponds to 5.8 Mo atom/$nm^2$ that is slightly higher than that for monolayer coverage (5.0 Mo atom/$nm^2$) but not so high that it forms crystalline species at the oxide stage, as described in a previous paper (22).

Figure 3 shows representative TEM images of $Mo/TiO_2$ catalysts sulfided in $H_2S/N_2$ at 573, 673, or 773 K after calcination in air. The catalyst sulfided at 573 K (Fig. 3a) had many edge-bonded $MoS_2$ clusters that were less than 2 nm long (indicated by a circle) but had no basal-bonded $MoS_2$ clusters. The number of Mo atoms estimated from the observed $MoS_2$ clusters in Fig. 3a was less than that expected from the Mo loading of 4.6%. This indicates high dispersion of $MoS_2$ clusters or insufficient sulfidation, similar to the results for the catalyst sulfided in $H_2S/H_2$. The catalyst sulfided at 673 K (Fig. 3b) had a relatively large number of edge-bonded $MoS_2$ clusters (indicated by a circle), resulting from the growth of small $MoS_2$ clusters that were not detected in the image, and a small number of basal-bonded $MoS_2$ clusters (indicated by a dotted circle). The catalyst sulfided at 773 K (Fig. 3c) mostly had large (>5 nm), multilayered basal-bonded $MoS_2$ clusters on the support (indicated by a dotted circle) but had relatively few edge-bonded $MoS_2$ clusters.

Figure 4 shows representative TEM images of $Mo/TiO_2$ catalysts sulfided in either $H_2S/H_2$ or $H_2S/N_2$ after calcination in $N_2$. The catalyst sulfided at 573 K in $H_2S/N_2$ (Fig. 4a) had edge-bonded $MoS_2$ clusters whose lengths were longer than those for the catalyst calcined in air (Fig. 3a). Comparison of the images of the catalysts calcined in $N_2$ with those of the corresponding catalysts calcined in air reveals the same trends; namely, the calcination atmosphere did not affect the orientation of the $MoS_2$ clusters, whereas the average length of the $MoS_2$ clusters was longer when the catalysts were calcined in $N_2$.

The $TiO_2$ support used in the present study was spherical with a *nonporous* structure. The TEM image presenting a whole particle, as shown in Figs. 2–4, gives the complete image of catalyst particles. Thus, we conclude that these TEM images are representative of the $MoS_2$ structures in the catalysts.

Table 1 summarizes the above TEM observation results, showing that the orientation of $MoS_2$ clusters on the support depended on the sulfidation conditions. Sulfidation of the catalyst in $H_2S/N_2$ enhanced the formation of edge-bonded $MoS_2$ clusters; however, these clusters changed their orientation to basal-bonded when sulfided at a temperature higher than 673 K. Sulfidation of the catalyst in $H_2S/H_2$ resulted in highly dispersed basal-bonded $MoS_2$ clusters. Increasing the sulfidation temperature in $H_2S/H_2$ caused aggregation of $MoS_2$ clusters, but less than the aggregation caused when the catalysts were sulfided in $H_2S/N_2$.

Figure 5 shows the effect of sulfidation conditions on the Mo 3d XPS spectra of $MoS_2/TiO_2$ catalysts calcined in air. As reported in numerous studies (26–30), when the degree of sulfidation was increased, two features, at 232.5 and 235.5 eV, which are assigned to $Mo^{6+}$ features (Mo $3d_{5/2}$ and Mo $3d_{3/2}$) from oxide species, shifted to 228.5 and 232.0 eV, which are assigned to $Mo^{4+}$ features from sulfide species. Simultaneously, S 2s features appeared at 226.0 eV.

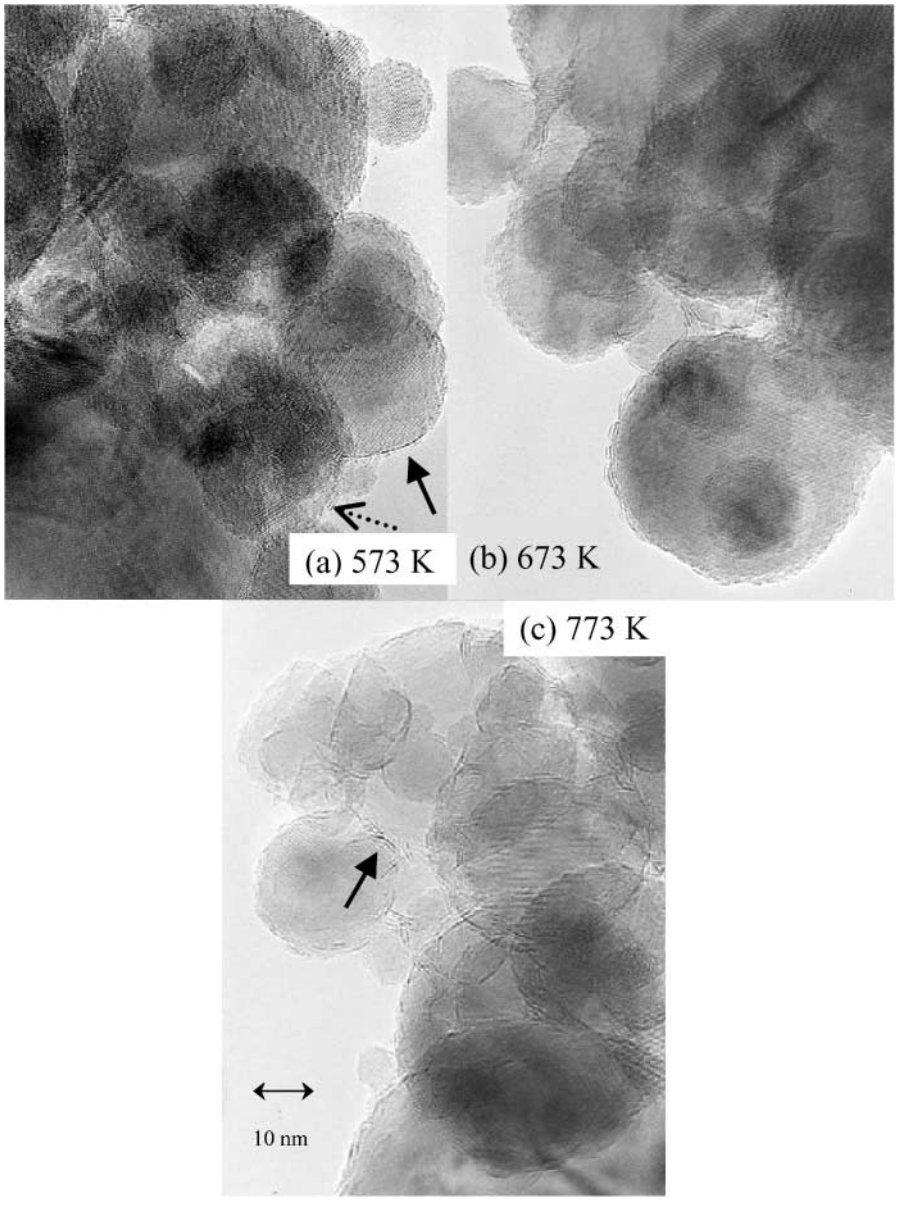


**FIG. 2.** Transmission electron microscopy (TEM) images of $MoS_2/TiO_2$ catalysts calcined in air and then sulfided in $H_2S/H_2$ at (a) 573 K (solid arrow indicates monolayered $MoS_2$ cluster and dotted arrow indicates two-layered $MoS_2$ cluster), (b) 673 K, and (c) 773 K (solid arrow indicates multilayered $MoS_2$ cluster). (×1,000,000.)

Asymmetric features observed in the spectra of the catalysts sulfided at low temperatures, typically those observed for the catalyst sulfided in $H_2S/H_2$ at 573 K (Fig. 5b), indicate the presence of $Mo^{5+}$ species, likely oxisulfide, in the transition stage from $Mo^{6+}$ to $Mo^{4+}$, as described in previous papers (28–30). In the Mo 3d spectra of $MoS_2/TiO_2$ catalysts calcined in $N_2$ (not shown here), changes similar to those of the $MoS_2/TiO_2$ catalysts calcined in air (Fig. 5) were observed, although the line widths of the features for the catalysts calcined in $N_2$ were slightly larger.

To quantitatively discuss the changes in Mo species, each spectrum was deconvoluted into seven peaks assigned to Mo $3d^{6+}_{5/2}$, Mo $3d^{6+}_{3/2}$, Mo $3d^{5+}_{5/2}$, Mo $3d^{5+}_{3/2}$, Mo $3d^{4+}_{5/2}$, Mo $3d^{4+}_{3/2}$, and S 2s. The curve fitting for each spectrum was done by using a least-squares method (included in the software package that accompanied the spectrometer, PHI 5500) with the following restrictions:

1. Peak area ratio of Mo $3d_{5/2}$/ Mo $3d_{3/2}$ was fixed at 3/2.
2. Peak energy difference between Mo $3d_{5/2}$ and Mo $3d_{3/2}$ was assumed constant.

Based on this curve fitting, the relative ratios of $Mo^{6+}$, $Mo^{5+}$, and $Mo^{4+}$ in the $MoS_2/TiO_2$ catalysts calcined in air were calculated and are shown in Fig. 6. As expected from Fig. 5, sulfidation in $H_2S/H_2$ at 573 K yielded nearly 80%

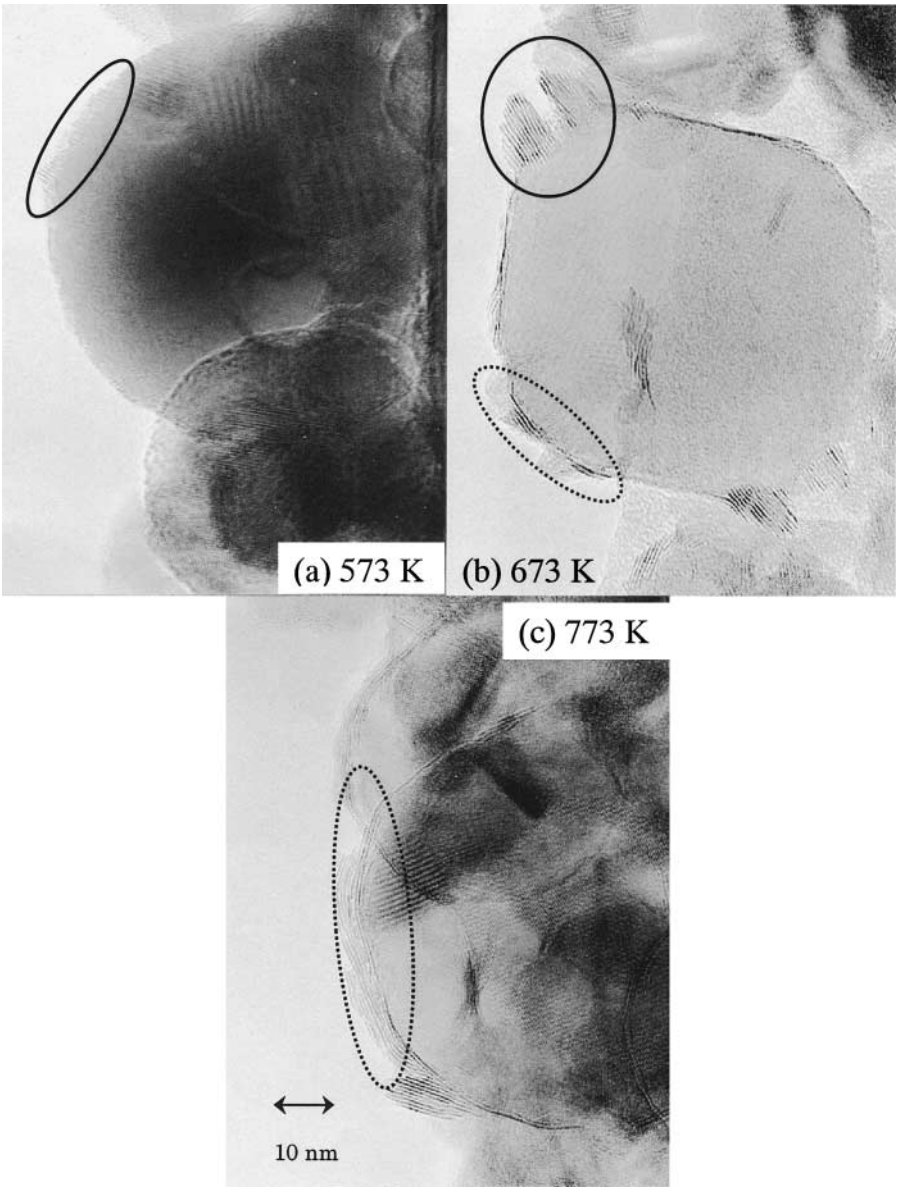


**FIG. 3.** Transmission electron microscopy (TEM) images of $MoS_2/TiO_2$ catalysts calcined in air and then sulfided in $H_2S/N_2$ at (a) 573 K (solid circle indicates edge-bonded $MoS_2$ cluster), (b) 673 K (solid circle indicates edge-bonded $MoS_2$ cluster and dotted circle indicates basal-bonded $MoS_2$ cluster), and (c) 773 K (dotted circle indicates basal-bonded $MoS_2$ cluster). (×1,000,000.)

$Mo^{4+}$, with the remaining assigned to $Mo^{5+}$. Sulfidation of the catalyst in $H_2S/N_2$ at 573 or 673 K resulted in higher ratios of $Mo^{4+}$ than sulfidation in $H_2S/H_2$, whereas at 773 K, the ratio remained unaffected. These results indicate that Mo oxide on $TiO_2$ was sulfided more rapidly in $H_2S/N_2$ than in $H_2S/H_2$.

Figure 7 shows the effect of sulfidation conditions on the S 2p XPS spectra of $MoS_2/TiO_2$ catalysts calcined in air. The doublets with a main peak at 161.8 eV observed in the sulfided catalysts were consistent with that of pure $MoS_2$. The major peak was assigned to S $2p_{3/2}$ of $S^{2-}$ in $MoS_2$, and the minor one assigned to S $2p_{1/2}$. In the spectra of the catalysts sulfided in $H_2S/H_2$ (Figs. 7a–7c), changes in the S 2p spectra corresponded to changes in the Mo 3d XPS spectra; namely, sulfidation at 573 K yielded mostly $MoS_2$-like species and the characteristics of the spectra approached those of pure $MoS_2$ with increasing sulfidation temperature.

The spectrum for the catalyst sulfided in $H_2S/N_2$ at 573 K (Fig. 7d) showed features different from those for the catalyst sulfided in $H_2S/H_2$ (Figs. 7a–7c). Figure 7 also shows the spectra of amorphous $MoS_3$ and elemental sulfur as references. Evidently, the spectrum of the catalyst sulfided in $H_2S/N_2$ at 573 K corresponded to the spectrum of $MoS_3$. According to previous studies (23, 31), the S $2p_{3/2}$

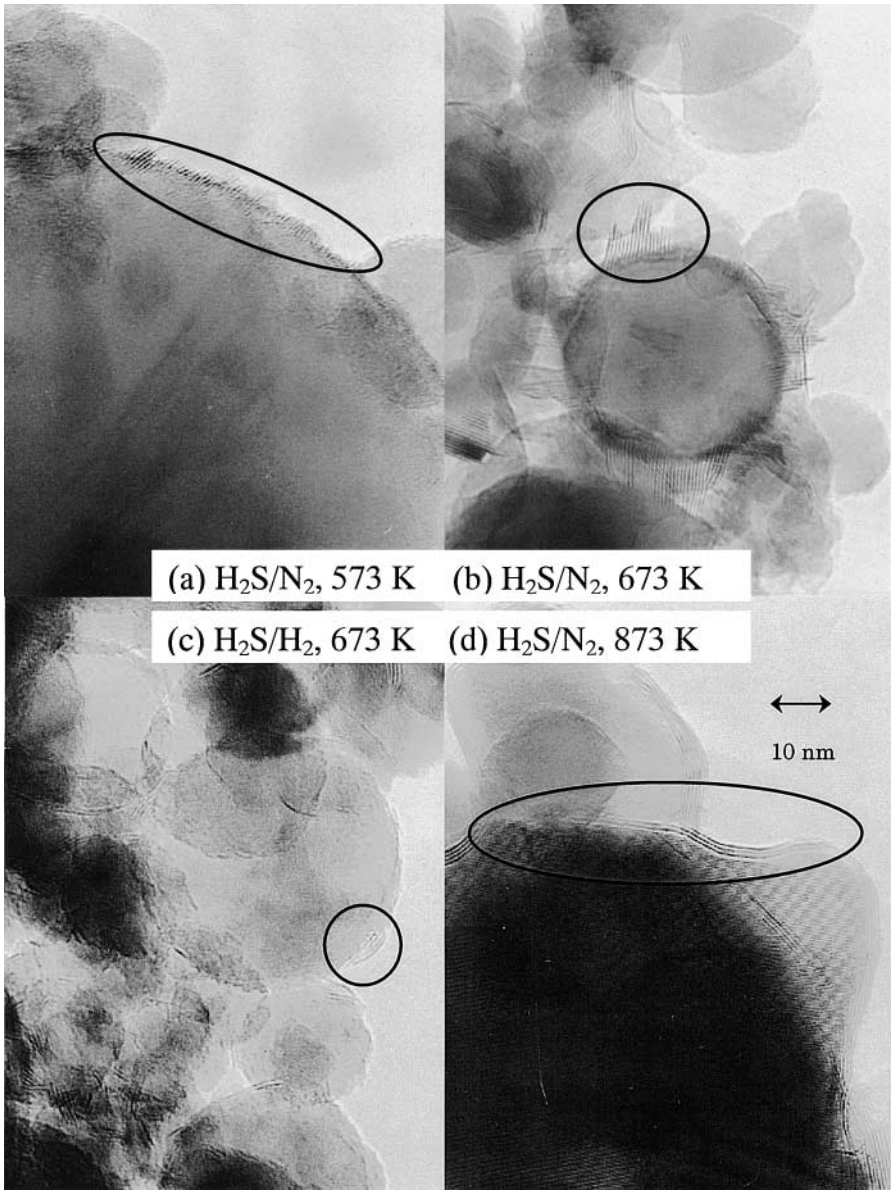


**FIG. 4.** Transmission electron microscopy (TEM) images of $MoS_2/TiO_2$ catalysts calcined in $N_2$ and then sulfided in (a) $H_2S/N_2$ at 573 K (circle indicates edge-bonded $MoS_2$ cluster), (b) $H_2S/N_2$ at 673 K (circle indicates edge-bonded $MoS_2$ cluster; this same image appeared in a previous paper (20)), (c) $H_2S/H_2$ at 673 K (circle indicates basal-bonded $MoS_2$ cluster), and (d) $H_2S/N_2$ at 873 K (circle indicates basal-bonded $MoS_2$ cluster). ($\times$1,000,000.)

binding energy of bridging $S_2^{2-}$ in $MoS_3$ is 162.9 $\pm$ 0.2 eV, those of terminal $S_2^{2-}$ and $S^{2-}$ in $MoS_3$ are 161.6 $\pm$ 0.2 eV, that of $S^0$ in elemental sulfur is 164.0 eV, and that of bridging $S^{2-}$ in $MoS_2$ is 161.8 eV. Based on these binding energies, the spectra in Fig. 7 were deconvoluted into the following three doublets (S $2p_{3/2}$ and S $2p_{1/2}$): S (HE) with S $2p_{3/2}$ at 164.0 $\pm$ 0.2 eV, S(ME) with S $2p_{3/2}$ at 162.9 $\pm$ 0.2 eV, and S (LE) with S $2p_{3/2}$ at 161.6 $\pm$ 0.2 eV. Thus, S (HE) is attributed to elemental sulfur, S (ME) to $MoS_3$, and S (LE) to $MoS_2$ and $MoS_3$. The fraction of each doublet was calculated by a curve fitting using the same procedure used for the Mo 3d spectra (see above) except that the peak area ratio of S $2p_{3/2}$/S $2p_{1/2}$ was fixed at 2.

Figure 8 shows the effect of sulfidation temperature on each of these fractions. The catalyst sulfided in $H_2S/N_2$ at 573 K contained 60% of the S (ME) assigned to bridging $S_2^{2-}$ in $MoS_3$. This fraction decreased with increasing sulfidation temperature and finally disappeared at 773 K. Figure 8 indicates that sulfidation of the catalyst in $H_2S/H_2$ also yielded $MoS_3$, although the fraction was smaller than that in the catalyst sulfided in $H_2S/N_2$. The observation of $MoS_3$ in the catalyst sulfided in $H_2S/H_2$ is consistent with

**TABLE 1**

**Formation Characteristics of $MoS_2/TiO_2$ Catalysts Calcined and Sulfided under Various Conditions (Revealed by TEM)**

| Calcination atmosphere | Sulfidation atmosphere | Sulfidation temperature (K) | Max. cluster length (nm) | Ave. cluster length (nm) | Number of layers | Ave. number of layers | Orientation |
|---|---|---|---|---|---|---|---|
| Air | $H_2S/H_2$ | 573 | | Few $MoS_2$ clusters were observed. | | | Basal bonding |
| | | 673 | | Few $MoS_2$ clusters were observed. | | | Basal bonding |
| | | 773 | 12 | 5.1 | 1–5 | 2.1 | Basal bonding |
| | $H_2S/N_2$ | 573 | | Few $MoS_2$ clusters were observed. | | | Edge bonding |
| | | 673 | 12 (Edge) | 5.7 (Edge) | 3–20 (Edge) | 9.3 (Edge) | Edge + basal |
| | | | 20 (Basal) | 8.0 (Basal) | 1–5 (Basal) | 2.0 (Basal) | |
| | | 773 | 60 (Basal) | 3.5 (Edge) | 3–9 (Edge) | 6.3 (Edge) | Edge + basal |
| | | | | 24.9 (Basal) | 1–9 (Basal) | 3.0 (Basal) | |
| $N_2$ | $H_2S/H_2$ | 573 | | Few $MoS_2$ clusters were observed. | | | Basal bonding |
| | | 673 | | Few $MoS_2$ clusters were observed. | | | Basal bonding |
| | | 873 | 40 | 15.5 | 1–10 | 3.2 | Basal bonding |
| | $H_2S/N_2$ | 573 | 7 | 3 | 1–20 | 4.8 | Edge bonding |
| | | 673 | 10 (Edge) | 6.2 (Edge) | 5–20 (Edge) | 10.4 (Edge) | Edge + basal |
| | | | 20 (Basal) | 9.7 (Basal) | 1–5 (Basal) | 2.1 (Basal) | |
| | | 873 | 100 | 33.2 | 1–15 | 3.1 | Basal bonding |

*Note.* The average length and average number of $MoS_2$ layers were obtained by averaging all the $MoS_2$ layers observed in three pictures with a magnification of 1,000,000 (15 cm × 20 cm).

previous results (32, 33) that report the formation of $MoS_3$ by sulfidation of the catalyst in $H_2S/H_2$ at low temperature. No spectra contained S (HE) from elemental sulfur; this is also consistent with previous results (27) that report the absence of the formation of elemental sulfur during the sulfiding of Mo oxide catalysts.

Based on the above discussion, sulfidation of oxide catalysts at first yielded $MoS_3$, which subsequently transformed into $MoS_2$ at higher temperature. Sulfidation of the catalyst in $H_2S/N_2$ is more likely to maintain the amorphous $MoS_3$ structures at higher temperature than does sulfidation in $H_2S/H_2$. Note that the exact fraction of $MoS_3$ is not the same as the fraction in Fig. 8, because S (LE) contains contributions from both $MoS_2$ and $MoS_3$.

The trends observed in the S 2p spectra of $MoS_2/TiO_2$ catalysts calcined in $N_2$ (not shown here) were similar to those observed in the S 2p XPS spectra of $MoS_2/TiO_2$ catalysts calcined in air (Fig. 7). The line width of each feature

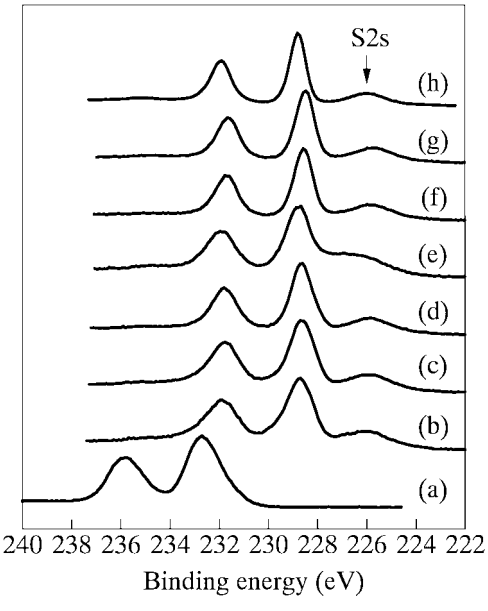


**FIG. 5.** Mo 3d X-ray photoelectron spectra of $MoS_2/TiO_2$ catalysts calcined in air (a) before sulfidation, and then after sulfidation in (b) $H_2S/H_2$ at 573 K, (c) $H_2S/H_2$ at 673 K, (d) $H_2S/H_2$ at 773 K, (e) $H_2S/N_2$ at 573 K, (f) $H_2S/N_2$ at 673 K, and (g) $H_2S/N_2$ at 773 K. (h) That of pure $MoS_2$.

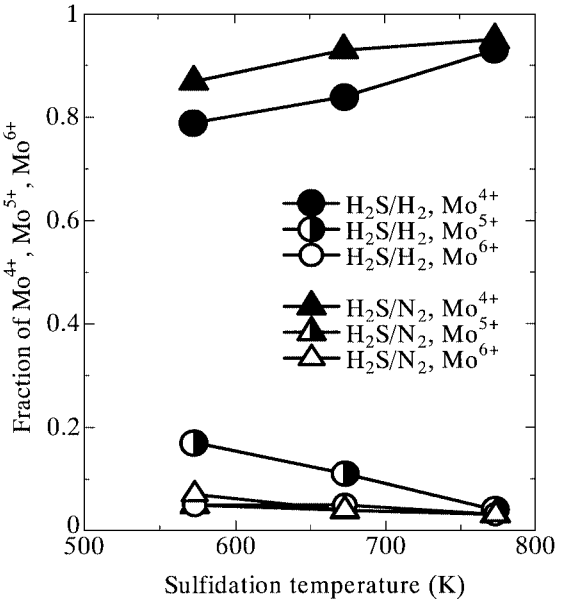


**FIG. 6.** Fraction of $Mo^{4+}$, $Mo^{5+}$, and $Mo^{6+}$ in $MoS_2/TiO_2$ catalysts calcined in air.

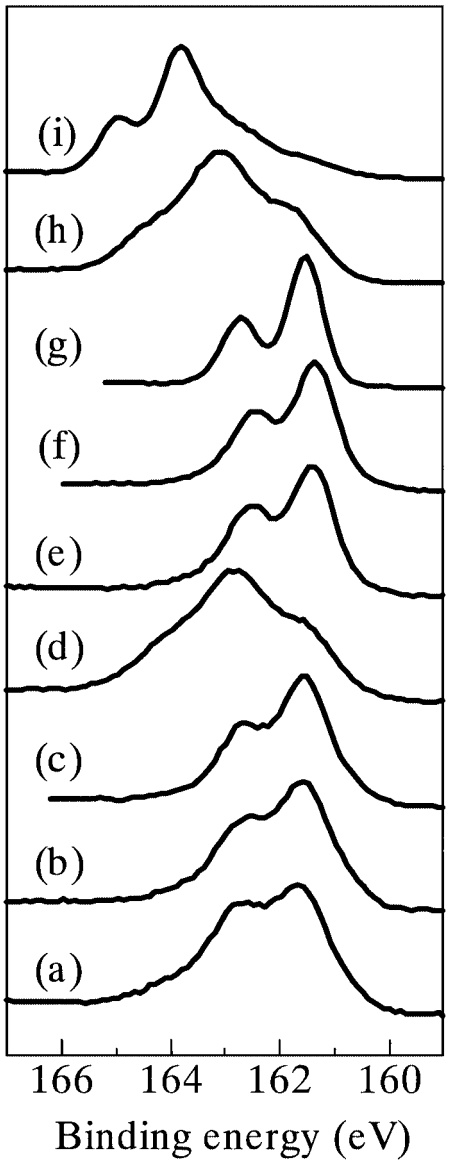


**FIG. 7.** S 2p X-ray photoelectron spectra of $MoS_2/TiO_2$ catalysts calcined in air and then sulfided in (a) $H_2S/H_2$ at 573 K, (b) $H_2S/H_2$ at 673 K, (c) $H_2S/H_2$ at 773 K, (d) $H_2S/N_2$ at 573 K, (e) $H_2S/N_2$ at 673 K, and (f) $H_2S/N_2$ at 773 K; that of (g) pure $MoS_2$, (h) $MoS_3$, and (i) elemental S.

in the spectrum for $MoS_2/TiO_2$ catalysts calcined in $N_2$ was larger than that of the corresponding feature of these catalysts calcined in air, similar to the correspondence between the Mo 3d spectra. Based on the XPS and TEM results, formation of edge-bonded $MoS_2$ clusters was likely related to the formation of $MoS_3$ during sulfidation. A short lifetime for $MoS_3$ during sulfidation in $H_2S/H_2$ presumably hindered the formation of edge-bonded $MoS_2$ clusters on $TiO_2$. Furthermore, $H_2$ in $H_2S/H_2$ possibly led to surface hydroxyl groups on $TiO_2$, which yielded basal-bonded $MoS_2$ clusters when sulfidation was done in $H_2S/H_2$.

Figure 9 shows the effect of sulfidation conditions on the NO uptake by $MoS_2/TiO_2$ catalysts calcined in air. The

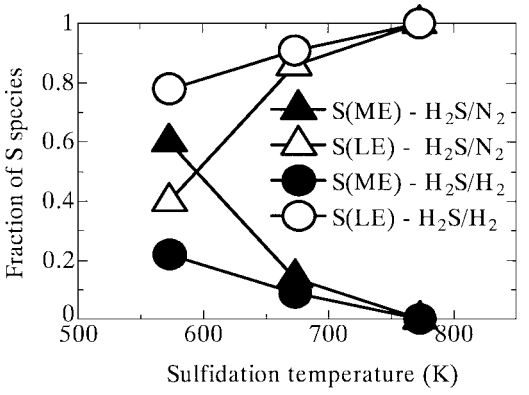


**FIG. 8.** Fraction of S (ME) and S (HE) in $MoS_2/TiO_2$ catalysts calcined in air. Closed triangle, S (ME) from $MoS_3$ in the catalyst sulfided by $H_2S/N_2$; open triangle, S (LE) from $MoS_2$ and $MoS_3$ in the catalyst sulfided by $H_2S/N_2$; closed circle, S (ME) from $MoS_3$ in the catalyst sulfided by $H_2S/H_2$; and open circle, S (LE) from $MoS_2$ and $MoS_3$ in the catalyst sulfided by $H_2S/H_2$.

dispersion of $MoS_2$ clusters was higher in the catalyst sulfided in $H_2S/H_2$ than in the catalyst sulfided in $H_2S/N_2$. In both sulfidation atmospheres, the dispersion decreased by increasing the sulfidation temperature. The NO/Mo values obtained for the present catalysts sulfided at 673 K (0.096 mol/mol for the catalyst sulfided in $H_2S/N_2$ and 0.145 mol/mol for the catalyst sulfided in $H_2S/H_2$) were almost the same or higher than that obtained for a laboratory-prepared $Mo/Al_2O_3$ catalyst sulfided at 673 K in $H_2S/H_2$ (0.095 mol/mol). Based on the TEM results, XPS results, and NO uptake measurements, the $MoS_2$ clusters in the catalysts calcined in air and sulfided in $H_2S/H_2$ at low temperature were highly dispersed and most were undetectable in the TEM images in Fig. 2.

The results of catalyst characterization are summarized as follows.

1. Sulfidation of the catalyst in $H_2S/N_2$ at the low temperature of 573 K yielded edge-bonded $MoS_2$ clusters. With

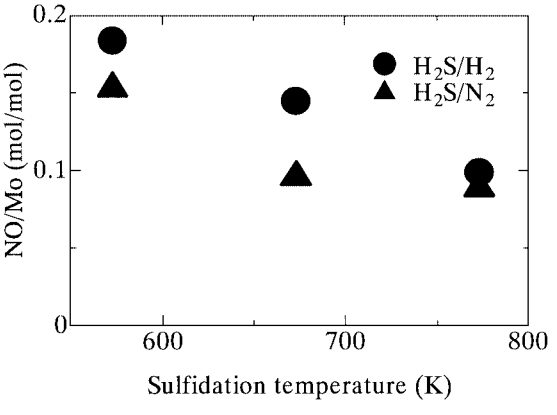


**FIG. 9.** NO uptake on the $MoS_2/TiO_2$ catalysts calcined in air and then sulfided under different atmospheres and temperatures.

increasing sulfidation temperatures, however, the edge-bonded clusters transformed to highly aggregated basal-bonded clusters.

2. Sulfidation of the catalyst in $H_2S/H_2$ yielded highly dispersed $MoS_2$ clusters. Although most of these clusters were undetectable in the TEM images, some of those that were detected showed preferential formation of basal-bonded $MoS_2$ clusters.

3. Calcination atmosphere did not affect the orientation of $MoS_2$ clusters on the support, either edge-bonded or basal-bonded, although calcination in air yielded higher dispersion of $MoS_2$ clusters after sulfidation than did calcination in $N_2$.

4. More than 80% of the Mo oxide transformed into Mo sulfide by sulfidation at 573 K. The effect of the remaining $Mo^{6+}$ species on the catalytic activity tests (discussed in the next section) can be assumed to be relatively small. The sulfided Mo species gradually aggregated with increasing sulfidation temperatures.

In a previous paper (20), we showed that edge-bonded $MoS_2$ clusters form on a $TiO_2$ support when the catalyst is calcined in $N_2$ and then sulfided in $H_2S/N_2$. Our current results indicate that sulfiding the catalyst in $H_2S/N_2$ was essential for the formation of edge-bonded clusters, whereas calcining in $N_2$ had no effect on such formation. Instead, although calcining in $N_2$ resulted in the formation of aggregated structures, this aggregation could have increased the possibility of detecting the edge-bonded $MoS_2$ clusters in the TEM observation in our previous study.

*Catalytic Activity*

Figure 10 compares the hydrogenation activities of the $MoS_2/TiO_2$ catalysts prepared under different conditions.

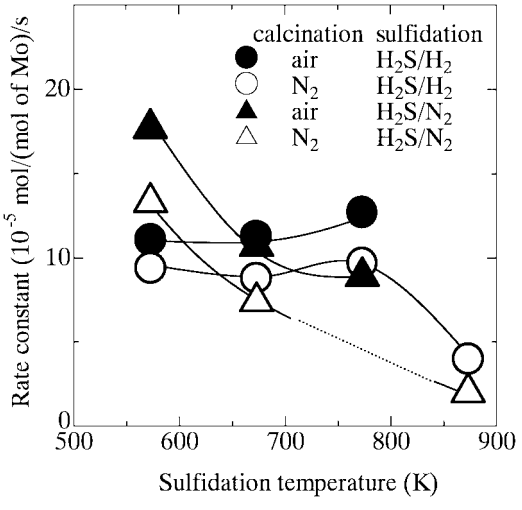


**FIG. 10.** Catalytic activity of $MoS_2/TiO_2$ catalysts calcined and sulfided under different calcination atmospheres, sulfidation atmospheres, and sulfidation temperatures.

The catalysts calcined in air showed higher activity than the corresponding catalysts calcined in $N_2$. Among the catalysts sulfided in $H_2S/N_2$, the catalytic activity gradually decreased with increasing sulfidation temperatures in each series of the catalysts calcined in air or $N_2$. In contrast, among the catalysts sulfided in $H_2S/H_2$, the catalytic activity increased with increasing sulfidation temperatures up to 773 K. The results show that the catalyst calcined in air and sulfided in $H_2S/N_2$ at 573 K yielded the highest activity.

Among the catalysts sulfided in $H_2S/N_2$, the change in the catalytic activity (Fig. 10) corresponded with that in the dispersion (Fig. 9). This indicates that catalytic activity decreased with a decrease in the number of active catalytic sites and that the turnover frequency (TOF) on the edge-bonded $MoS_2$ clusters was relatively independent of the dispersion. In contrast, the catalytic activity of the catalyst sulfided in $H_2S/H_2$ increased with increasing sulfidation temperatures, despite a decrease in the dispersion (Fig. 9). The TOF on the basal-bonded $MoS_2$ clusters increased with increasing sulfidation temperatures. This increase is presumably due to the decrease in the electronic interaction between the basal-bonded $MoS_2$ clusters and $TiO_2$ support, corresponding to the transformation of single-layered $MoS_2$ clusters to multilayered $MoS_2$ clusters shown in Fig. 1. This is in good agreement with the increase in the catalytic activity of Co–Mo sulfide catalysts from Co–Mo–S(I) to Co–Mo–S(II), as reported in the literature (7–12). Furthermore, the TOF on the edge-bonded $MoS_2$ clusters was higher than that on the basal-bonded $MoS_2$ clusters, because the number of active catalytic sites estimated by using the NO uptake for the edge-bonded clusters was smaller than that for the edge-bonded clusters at each sulfidation temperature (Fig. 9).

Sulfidation of the catalyst in $H_2S/N_2$ at a temperature higher than 673 K, however, yielded rapid aggregation of $MoS_2$ clusters. As a result, the activity of the catalyst sulfided in $H_2S/H_2$ was superior to that of the catalyst sulfided in $H_2S/N_2$ when the sulfidation temperature was 673 K. Edge-bonded $MoS_2$ clusters probably aggregate more easily than do basal-bonded $MoS_2$ clusters, because edge-bonded clusters have weaker electronic interaction with the support.

Numerous studies have reported that the catalytic activities of $TiO_2$-supported $MoS_2$ catalysts are superior to those of $Al_2O_3$-supported catalysts (34–39). Consequently, numerous discussions on the possible reasons for this superiority of $TiO_2$-supported catalysts have been reported, although no definite conclusion has been reached. One possible reason for the superior activity is that the formation of edge-bonded $MoS_2$ clusters might contribute to the high activity of $TiO_2$-supported catalysts.

Our current results reveal, however, that edge-bonded clusters are not as stable as basal-bonded clusters. In addition, populating the edge sites of a $MoS_2$ cluster with Co is essential for practical preparation of catalysts. Further

studies are needed to apply the edge-bonded clusters discussed in our study to industrial catalysts.

## CONCLUSION

Formation and catalytic properties of edge-bonded $MoS_2$ clusters on $TiO_2$ supports were studied. The following conclusions were obtained.

1. Edge-bonded $MoS_2$ clusters formed on $TiO_2$ supports by sulfiding the oxide precursor in $H_2S/N_2$ at low temperatures, such as 573 and 673 K. The edge-bonded $MoS_2$ clusters transformed to aggregated basal-bonded clusters by sulfidation at high temperatures, such as 773 K.

2. In the hydrogenation of 1-methylnaphthalene, edge-bonded $MoS_2$ clusters on $TiO_2$ showed a higher turnover frequency than did basal-bonded $MoS_2$ clusters on $TiO_2$.

## REFERENCES


1. Houalla, M., Broderick, D., deBeer, V. J. H., Gates, B. C., and Kwart, H., Preprint of Am. Chem. Soc. Div. Petroleum Chem., **22**, 941 (1977).
2. Katti, S. S., Westerman, D. W. B., Gates, B. C., Youngless, T., and Petrakis, L., *Ind. Eng. Chem. Process Des. Dev.* **23**, 773 (1984).
3. Kabe, T., Ishihara, A., and Zang, Q., *Appl. Catal. A* **97**, L1 (1993).
4. Topsøe, H., Clausen, B. S., Candia, R., Wivel, C., and Mørup, S., *J. Catal.* **68**, 433 (1981).
5. Topsøe, H., Clausen, B. S., and Massoth, F. E., *in* "Hydrotreating Catalysis" (J. R. Anderson and M. Boudart, Eds.), Vol. 11, p. 162. Springer-Verlag, Berlin/Heidelberg, 1996.
6. Candia, R., Sørensen, O., Villadsen, J., Topsøe, N., Clausen, B. S., and Topsøe, H., *Bull. Soc. Chim. Belg.* **93**, 763 (1984).
7. Bouwens, S. M. A. M., van Zon, F. B. M., van Dijk, M. P., van der Kraan, A. M., de Beer, V. H. J., van Veen, J. A. R., and Koningsberger, D. C., *J. Catal.* **146**, 375 (1994).
8. Topsøe, H., Clausen, B. S., Topsøe, N.-Y., and Zeuthen, P., *Stud. Surf. Sci. Catal.* **53**, 77 (1990).
9. Ramirez, J., Fuentes, S., Diaz, G., Vrinat, M., Breysse, M., and Lacroix, M., *Appl. Catal.* **52**, 211 (1989).
10. Eijsbouts, S., *Appl. Catal. A* **158**, 53 (1997).
11. Brown, V. M., Louwers, S. P. A., and Prins, R., *Catal. Today* **10**, 345 (1991).
12. Louwers, S. P. A., Craje, M. W. J., van der Kraan, A. M., Geantet, C., and Prins, R., *J. Catal.* **144**, 579 (1993).
13. Whitehurst, D. D., Isoda, T., and Mochida, I., *Adv. Catal.* **42**, 345 (1998).
14. Vrinat, M., Breysse, M., Geantet, C., Ramirez, J., and Massoth, F., *Catal. Lett.* **26**, 25 (1994).
15. Daage, M., and Chianelli, R. R., *J. Catal.* **149**, 414 (1994).
16. Pratt, K. C., Sanders, J. V., and Christov, V., *J. Catal.* **124,** 416 (1990).
17. Hayden, T. F., and Dumesic, J. A., *J. Catal.* **103**, 366 (1987).
18. Stockmann, R. M., Zandbergen, H. W., van Langeveld, A. D., and Moulijn, J. A., *J. Mol. Catal. A* **102**, 147 (1995).
19. Sakashita, Y., and Yoneda, T., *J. Catal.* **185**, 487 (1999).
20. Sakashita, Y., Araki, Y., Honna, K., and Shimada, H., *Appl. Catal. A* **197**, 247 (2000).
21. Wang, L., and Hall, K., *J. Catal.* **77**, 232 (1982).
22. Kim, D. S., Kurusu, Y., Wachs, I. E., Hardcastle, F. D., and Segawa, K., *J. Catal.* **120**, 325 (1989).
23. Weber, Th., Muijsers, J. C., and Niemantsverdriet, J. W., *J. Phys. Chem.* **99**, 9194 (1995).
24. Chang, C. H., and Chan, S. S., *J. Catal.* **72**, 139 (1981).
25. Eijsbouts, S., and Heinerman, J. J. L., *Appl. Catal. A* **105**, 53 (1993).
26. Brinen, J. S., and Armstrong, W. D., *J. Catal.* **54**, 57 (1978).
27. Li, C. P., and Hercules, D. M., *J. Phys. Chem.* **88**, 456 (1984).
28. Makovsky, L. E., Stencel, J. M., Brown, F. R., Tischer, R. E., and Pollack, S. S., *J. Catal.* **89**, 334 (1984).
29. Jepsen, J. S., and Rase, H. F., *Ind. Eng. Chem. Prod. Res. Dev.* **20**, 467 (1981).
30. Jong, A. M., Borg, H. J., van Ijzendoorn, L. J., Soudant, V. G. F. M., de Beer, V. H. J., van Veen, J. A. R., and Niemantsverdriet, J. W., *J. Phys. Chem.* **97**, 6477 (1993).
31. Muijsers, J. C., Weber, Th., van Hardeveld, R. M., Zandbergen, H. W., and Niemantsverdriet, J. W., *J. Catal.* **157**, 698 (1995).
32. Payen, E., Kasztelan, S., Houssenbay, S., Szymanski, R., and Grimblot, J., *J. Phys. Chem.* **93**, 6501 (1989).
33. de Boer, M., van Dillen, A. J., Koningsberger, D. C., and Geus, J. W., *J. Phys. Chem.* **98**, 7862 (1994).
34. Matsuda, S., and Kato, A., *Appl. Catal.* **8**, 149 (1983).
35. Ng, K. Y. S., and Gulari, E., *J. Catal.* **95**, 33 (1985).
36. Shimada, H., Sato, T., Yoshimura, Y., Hiraishi, J., and Nishijima, A., *J. Catal.* **110**, 275 (1988).
37. Ramirez, J., Fuentes, S., Diaz, G., Vrinat, M., Breysse, M., and Lacroix, M., *Appl. Catal.* **52**, 211 (1989).
38. Okamoto, Y., Maezawa, A., and Imanaka, T., *J. Catal.* **120**, 29 (1989).
39. Luck, F., *Bull. Chim. Soc. Belg.* **100**, 781 (1991).